Electronic Supplementary Information (ESI) for Predictability of silver nanoparticle speciation and toxicity in ecotoxicological media

Jan Köser,[a] Maria Engelke,[a] Martin Hoppe,[b] André Nogowski,[c] Juliane Filser,[a] and Jorg Thöming[a]

1 Preparation of silver standards ($AgNO_3$)

Primary silver standard solutions were prepared following the norm[1] using silver nitrate in diluted nitric acid (1 %) in the concentrations 10 g Ag/L to 10 mg Ag/L. These solutions were stable for longer periods of time in the dark. The reliability of the silver content measurement in the test media using GF-AAS was investigated by measuring mixtures of silver standard solutions and test media covering four orders of magnitude, each comprising four concentrations, from 50 μg Ag/L up to 200 mg Ag/L. To achieve this, secondary silver standard solutions (1 mL) were prepared before each set of experiments by adding volumes of 50 μL, 100 μL, 150 μL and 200 μL of silver standards to the appropriate volumes of nitric acid (1 %). Mixtures of 100 μL test medium and 10 μL of the secondary silver standard solutions were then treated and measured by GF-AAS according the digestion and dilution procedure described below.

2 Sample preparation for GF-AAS measurement

The described method was based on Luther *et al.*[2] modified by using *aqua regia*. The sample preparation followed the scheme shown in Figure S1 using disposable containers (Eppendorf tubes, PP, 1.5 mL) to reduce contamination risks. Basic sample volume was 100 μL. For longer storage durations before the actual measurement samples were stabilised by adding 10 μL of HNO_3 (1 %).

Commonly, AgNP dispersions are acid digested and then diluted in acidified ddH_2O using nitric acid[3–7], but preliminary results proved that this approach was not applicable in this study (e.g. GF-AAS recovery of $\approx$ 53 % for $AgNO_3$, 8 mg Ag/L, in test medium for HepG2).

Hence, *aqua regia* digestion was chosen due to the wide range of chloride content in the test media. The high excess of chloride prevents precipitation of silver chloride ($AgCl_s$) and ensured the formation of soluble higher silver chloride complexes ($[AgCl]_{aq}$, $[AgCl_2]^-_{aq}$, ...)[8,9]. Digestion was done by adding 80 μL of concentrated HCl (37 %) and 20 μL of concentrated HNO_3 (65 %) according the procedure reported by[10]. Thus, the volume ratio of HCl to HNO_3 is 4:1, which amounts to a molar ratio of $\approx$ 3:1. After vortexing for approx. 5 s and centrifugation for 30 s at $\approx 6,700$ g the opened samples were placed in a thermostat and digested at 56 °C overnight. In case the samples still contained liquid after this procedure, the temperature was increased to 95 °C. After cooling the dry samples to room temperature 1 mL of diluted *aqua regia* (100 mL consisted of 11 mL conc. HNO_3 (65 %) and 44 mL conc. HCl (37 %) and approx. 45 mL ddH_2O) was added. After vortexing for 30 s and centrifugation for 5 min at $\approx 6,700$ g part of the supernatant (700 μL) was cautiously transferred to the AAS sampler vial. In case the estimated silver concentration was higher than the upper limit of the working range (20 μg Ag/L) subsequent dilution steps of the supernatant using the diluted *aqua regia* solution were performed until the working range was reached (see example in Figure S1). Using the above described digestion procedure the quantification limit was increased to approx. 5.6 μg Ag/L (related to the untreated sample, see description below). The presented method led to high recovery for $AgNO_3$ in the studied test media covering 4 orders of magnitude

[a] *UFT - Centre for Environmental Research and Sustainable Technology, University of Bremen, Leobener Straße 6, D-28359 Bremen, Germany. E-mail: koeser@uni-bremen.de*
[b] *BGR - Federal Institute for Geosciences and Natural Resources, Stilleweg 2, D-30655 Hannover, Germany*
[c] *Technical University of Dresden, Institute of Process Engineering and Environmental Technology, D-01062 Dresden, Germany*

from 5 μ g/L to 200 mg/L Ag (see Figure S2).

3 Determination of silver content by GF-AAS

Total silver concentration was quantified by graphite furnace atomic absorption spectrometry (GF-AAS) using an Unicam 989 QZ AA Spectrometer (Unicam, Cambridge, UK) with GF-90 plus furnace and FS-90 plus autosampler after *aqua regia* digestion. Following detailed measurement conditions were chosen: Light source was a Perkin-Elmer hollow cathode lamp for silver powered with 9 mA (90 % of maximum power). The transmitted light was detected by photo multiplier tube at wavelength 328.1 nm. The slit width was adjusted to 0.5 nm. Background absorption was corrected for using the Zeeman effect.

The injected sample volume was set to 12 μL. Per injection additional 3 μL of 1 g Pd/L palladium nitrate ($Pd(NO_3)_2$) in nitric acid 1 % served as matrix modifier. The used graphite furnace tube was coated and equipped with a L'vov platform. The temperature program for the graphite furnace is given in Table S1 and was based on the recommendation of Butcher *et al.* 1998, p 51[11]. Each sample was measured in 3 replicates. The absorption signal was recorded as peak area (A·s). In the working range of 0.5 μg Ag/L to 20 μg Ag/L the signal was linearly correlated to the silver concentration of the $AgNO_3$ standard with a correlation coefficient of $r^2 > 0.995$. The characteristic mass was $m_0 \approx 2.5$ pg, calculated according to Slavin *et al.*[12]. Following MacDougall *et al.*[13] the quantification limit in this configuration was estimated to be 0.56 μg Ag/L (and the detection limit 0.17 μg Ag/L).

4 Data evaluation including error propagation

A calibration using a silver standard ($AgNO_3$, 20 μg Ag/L in HNO_3, 1 %, w/w) was recorded prior to each measurement. The controlling software was set to 4 standards (5 μg Ag/L - 20 μg Ag/L). The absorption signal S was corrected for the blank value S_b and then plotted vs. the nominal Ag concentration. The data was evaluated using linear regression (Microsoft Excel 2007) omitting the intercept. The sample concentration c was calcutated using the linear term $c = m(S-S_b)D_F$ with the dilution factor $D_F = \prod_{i=1}^{n} D_{F,n}$.

The uncertainty Δc was estimated using error propagation according to Ku[14] from the uncertainties of the signal ΔS, the blank value ΔS_b, the slope of regression Δm, the sample volume ΔV and the uncertainties of the dilution factors of each dilution step $\Delta D_{F,n}$. The relative uncertainty of the slope was estimated following the method of least squares[15] to be 5 %. The relative uncertainty of each dilution step was 2 %, calculated from relative volume uncertainty 1.4 %[16] of the used variable pipettes (10 - 100 μL & 100 - 1000 μL, Reference, Eppendorf, Hamburg, Germany). The relative uncertainty of sample volume ΔV was also estimated to 2 %. For the measurement of samples with low silver content (5 - 200 μg Ag/L) the following equation (1) applies for the estimation of Δc. For higher silver contents further dilution steps ($D_{F,2}$ and $D_{F,3}$) were conducted and were therefore considered by extending the equation (1) (see also Figure S1).

$$\Delta c = \sqrt{\left(\frac{\partial c}{\partial m}\right)^2 \Delta m^2 + \left(\frac{\partial c}{\partial S}\right)^2 \Delta S^2 + \left(\frac{\partial c}{\partial S_b}\right)^2 \Delta S_b^2 + \left(\frac{\partial c}{\partial V}\right)^2 \Delta V^2 + \left(\frac{\partial c}{\partial D_{F,1}}\right)^2 \Delta D_{F,1}^2 + \ldots} \quad (1)$$

Table S1 Temperature program of the graphite furnace during AAS measurements. The actual measurement takes place at the atomisation step at 1900 °C.

Cycle step	**Tube temperature** [°C]	**Hold time** [s]	**Temperature ramp** [°C/s]	**Argon flow** [L/min]
Dry step 1	120	15	10	0.2
Dry step 2	160	15	10	0.2
Pyrolysis	600	15	150	0.2
Cool down	200	15	10	0.2
Atomise	1900	5	–	0 (measurement)
Clean	2500	3	0	0.2

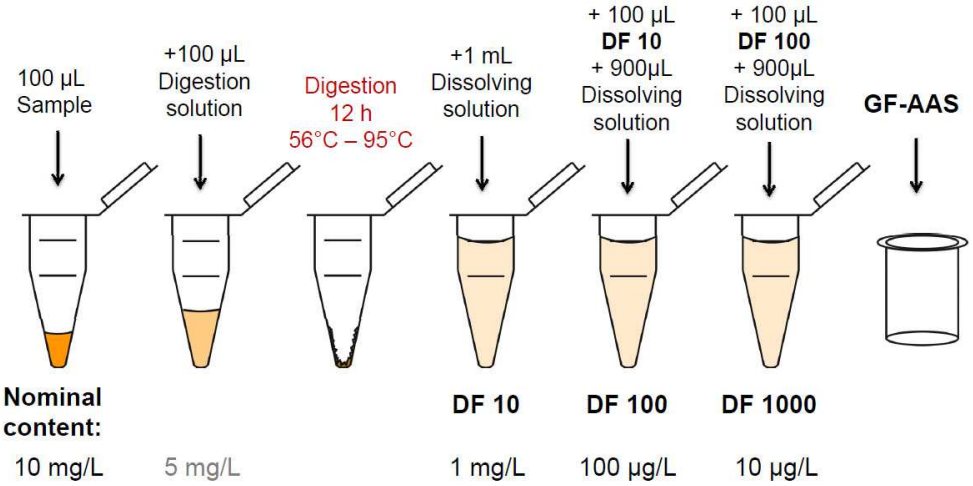

Fig. S1 Sample preparation for GF-AAS: Dilution sequence shown for a sample with the silver content of 10 mg/L.

Table S2 Comparison of silver contents in mg/L measured by GF-AAS, with ICP-OES and evaluation of the plasmon resonance in UV-Vis spectra.

Sample (nominal Ag content) ([mg Ag/L])	GF-AAS *aqua regia* digestion [mg Ag/L]	ICP-OES nitric acid digestion [mg Ag/L]	UV-Vis (d50,3) plasmon resonance evaluation [mg Ag/L]
NanoXact (20)	14.9 ± 0.2	14.1 ± 0.1	14.2 (39.0 nm)
NM-300K (20)	15.0 ± 0.3	14.5 ± 0.4	15.6 (51.4 nm)
$AgNO_3$ (20)	18.8 ± 0.9	–	–

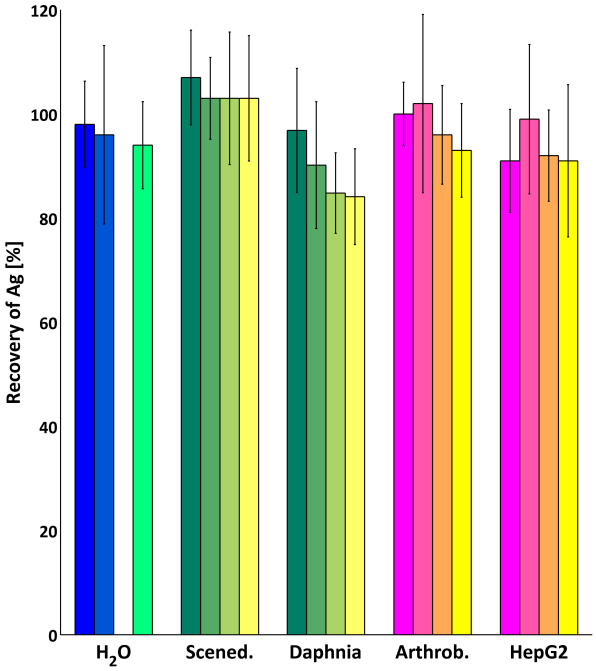

Fig. S2 Recovery for silver nitrate solutions in biological test media using GF-AAS and sample preparation with *aqua regia*. The concentration range covers 4 orders of magnitude from 5 μg Ag/L to 200 mg Ag/L ($n \geq 3$). In each group of bars the data is shown for the dilution factors 1, 10, 100 up to 1000 (from left to right). The errorbars represent the uncertainties estimated from equation (1).

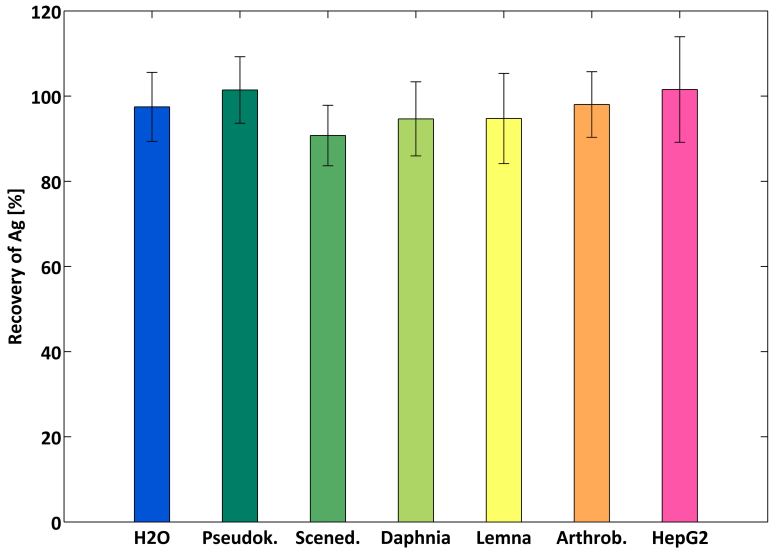

Fig. S3 Recovery for 7.9 mg/L NM-300K silver nanoparticles in biological test media (DF 1000, $n \geq 4$ except for Scened. $n = 2$). The errorbars represent the uncertainties estimated from equation (1).

Table S3 Silver content of NM-300K stock dispersion in mg/L measured by ICP-OES ($n = 3$). Uncorrected nominal silver content is 101.6 mg/L.

Vial No.	date	c_{Ag} [mg Ag/L]	recovery [%]
6125	07/25/2011	74.3 ± 1.0	73.2 ± 1.0
6495	11/07/2011	78.0 ± 0.5	76.8 ± 0.5
6496	11/28/2011	75.2 ± 0.8	74.0 ± 0.8
6480	01/09/2012	77.9 ± 0.6	76.7 ± 0.6
6481	02/06/2012	78.1 ± 1.0	76.8 ± 1.0
6566	06/11/2012	80.8 ± 0.6	79.6 ± 0.6
7018	11/07/2012	84.2 ± 0.8	82.8 ± 0.8
7046	01/17/2013	86.0 ± 2.3	84.6 ± 2.2
7047	02/07/2013	89.1 ± 0.3	87.7 ± 0.3
	mean $\pm$ stdev.	80.4 ± 5.0	79.1 ± 5.0

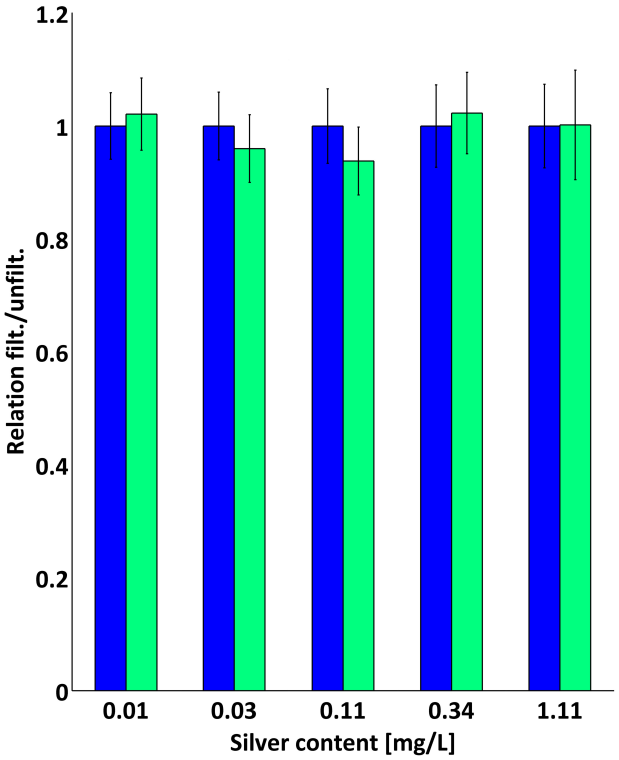

Fig. S4 Relation of membrane filtered (MF) silver nitrate samples (in HNO_3 1 %) to directly measured samples ($n = 2$, except MF for 0.03 mg/L, $n = 1$). The errorbars represent the uncertainties estimated from equation (1).

5 Determination of colloidal properties

Hydrodynamic diameters (HDD) were determined by dynamic light scattering (DLS) using a Beckman-Coulter DelsaNanoC (Beckman Coulter, Krefeld, Germany). This device features a diode laser (30 mW, $\lambda_0 = 658$ nm) and is able to measure the scattered at scattering angles of 15° and 165°. The DLS experiments were carried out at the backscattering angle 165°. The scattered light is detected using a photo multiplier tube and is analysed with a digital correlator. A sample volume of 2.5 mL was filled in Sarstedt fluorescence cuvettes (polystyrene, $d = 1$ cm, Sarstedt, Nümbrecht, Germany) and was thermostated at $t = 25$°C in the device for 15 min before the measurement time of 600 s (10 repetitions each 60 s). The samples were measured in three independent replicates. For the evaluation of the correlation functions $g^{(2)}$ the properties of pure water for the refractive index $n(658\text{nm}, 25°\text{C}) = 1.3328$ and for the viscosity $\eta(25°\text{C}) = 0.8878$ cP were used as given by the Beckman Coulter Software. The non-negative-least-square (NNLS) algorithm was used to calculate the intensity weighted HDD distribution. The first mode of the HDD distribution was recorded. Results for NM-300K dispersions are given in Figure S5. Please note that the media were filtered using 0.45 μm RC syringe filters (CS Chromatographie Service, Langerwehe, Germany) before preparing the dispersions.

The zetapotential was measured by electrophoretic light scattering (ELS) also using the Beckman-Coulter DelsaNanoC. A sample volume of 5 mL was filled in a Flow Cell and equilibrated with same conditions described for DLS above. Here the measurement was done at the scattering angle of 15°. The scattered light was recorded at 5 different positions for 40 s in the cell and corrected for electroosmotic flow. The measurements were done with 3 repetitions and 3 independent replicates. For the evaluation additionally to refractive index and viscosity the relative permittivity of pure water was used $\varepsilon = 78.3$ as given by the Beckman Coulter software. The scattered light is evaluated using a Lorentz fit function assuming one frequency peak. To calculate the zetapotential the Smoluchowski equation was used. The Henry function was set to $f(\kappa\alpha) = 1.5$, which is valid for ionic strengths $I \geq 10$ mM. Results for NM-300K are shown in Figure S6. In addition to the zetapotential, the electric conductivity was recorded. The pH of the samples was measured using a pH electrode (Voltcraft PH-100ATC, Conrad Electronic AG, Wollerau, Switzerland).

Additionally the UV-Vis spectra of the samples were recorded using a CADAS 200 spectral photometer (Hach Lange, Berlin, Germany). The wavelength range 350 - 800 nm was chosen to include the plasmon resonance of the NM-300K near 410 nm and peaks of bigger AgNP from possible agglomeration. The spectra were measured in 3 replicates corrected for the absorption of the respective media and are given in Figure S7 as mean of the 3 replicates.

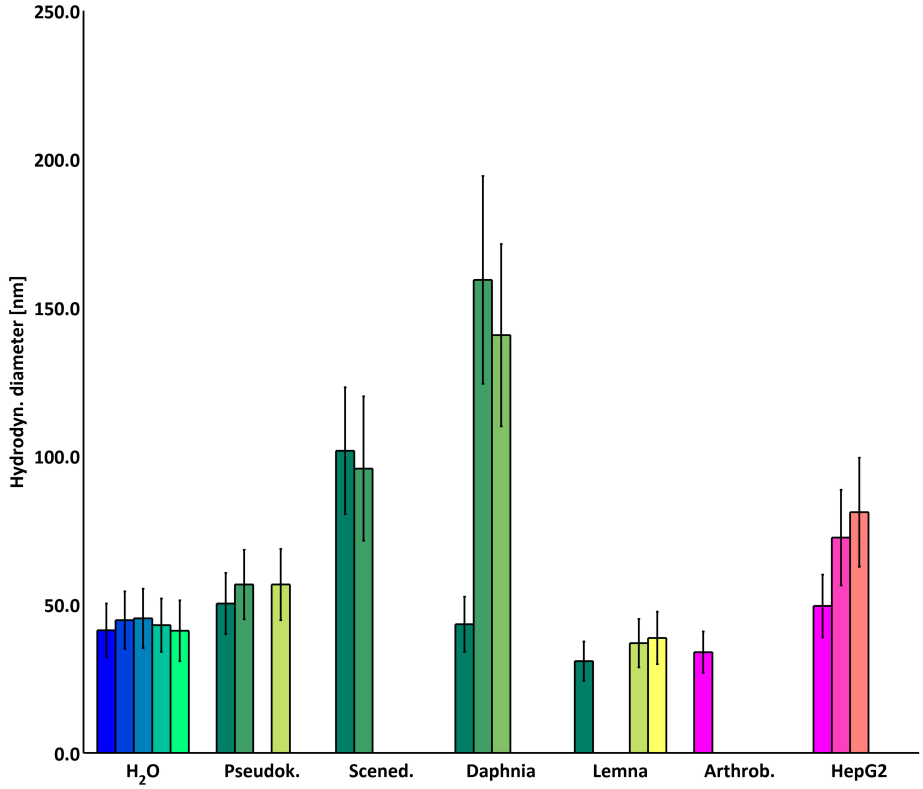

Fig. S5 Hydrodynamic diameter of AgNP NM-300K in test media measured by DLS ($n = 3$) at different time points. The dispersions in water were measured at day 0 (2 h), 1, 2, 3 and 7. For the test media the measurements were conducted at the beginning of the test period (2 h), the respective test end (see main text Table 1) and at an intermediate time point (Pseudok. 1 d, Daphnia 1 d, Lemna 3 d, HepG2 1 d). For Scenedesmus only data for day 0 and 1 were recorded.

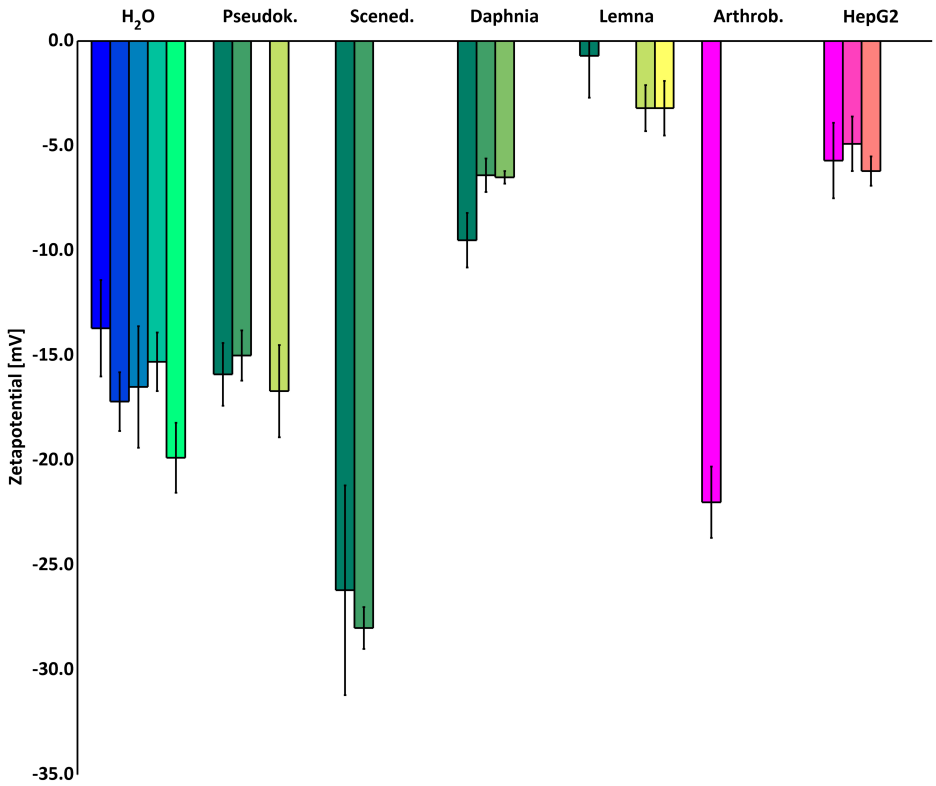

Fig. S6 Zetapotential of AgNP NM-300K in test media measured by ELS ($n = 3$) at different time points (same as for DLS, Figure S5).

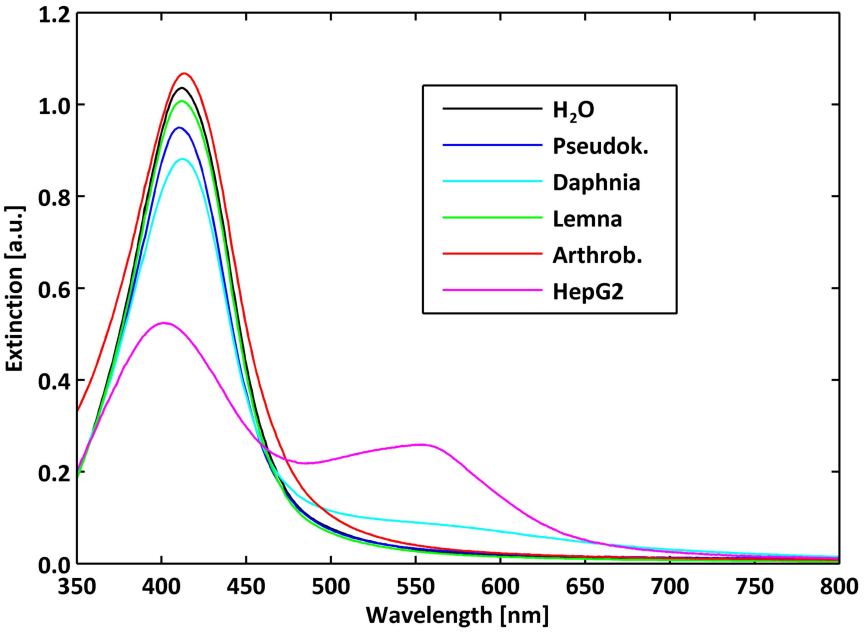

Fig. S7 UV-Vis spectra of AgNP NM-300K in test media ($n = 3$) at the end of the respective test periods (see main text Table 1).

Table S4 Species concentrations of the test media used as input parameters for the numerical speciation calculations. The concentrations were calculated according the test protocols (see main text section 2.8). The entry for cysteine (proteins) is used in the speciation calculation as proxy for the BSA Ag^+ binding and is calculated assuming $n = 9$ available cysteine groups of BSA and approximating the protein Ag^+ interaction with the Ag^+ BSA data. Only components are shown here, that are listed in the modified database minteq.v4 of the software PHREEQCi (v.3)[17] (see main text section 2.9).

[mmol/L]	Lemna	Pseudok.	Elendt M7	Scened.	Arthrob.	HepG2
pH	5.5	8.1	7.0	6.4	7.20	6.8
Cl^-	0.01025	0.64696772	4.078	8.247	11.41	109.4264
Ca^{2+}	1.25	0.122	1.998	0.1		0.42372
Na^+	0.00928	0.5955958	0.8658	13.065	11.41	137.7429
CO_3^{2-}		0.64696772	0.7714			27.8646
SO_4^{2-}	0.41063	0.0609	0.5038	1.0398		0.198
Mg^{2+}	0.41	0.1199	0.5002	1.0142		0.198
K^+	4.266	0.00919	0.081	8.012		5.3654
SiO_4^{4-}			0.0352			
H_3BO_3	0.00194	0.00299	0.0116	0.0080863		
EDTA	0.00446	0.000269	0.006716	0.027661		
Fe^{2+}			0.0036	0.024812		
Fe^{3+}	0.00281	0.000237				
NO_3^-	5.96		0.003224	8.012		0.8469
PO_4^{3-}	0.733	0.00919	0.0021	3.973		5.6354
Li^+			0.0018			
Mn^{2+}	0.00091	0.0021	0.00046	0.0025265		
Rb^+			0.00015			
Sr^{2+}			0.00014			
Zn^{2+}	0.00063	2.20E-05	0.000095	0.00069551		
MoO_4^{2-}	0.00018	2.89E-05	0.000065	0.001133		
Co^{2+}		6.30E-06	0.000042			
Br^-			0.000039			
Cu^{2+}		6.00E-08	0.000025			
J^-			0.00002			
SeO_4^{2-}			0.000013			
NH_4^+		0.64696772	0.000005	0.000971		
VO_3^-			0.000005			
Glucose					3.70	11.1
Glutamate						0.1359
Glycine						0.1332
Cysteine (free)						0.413
Proteins [g/L]					2	80
Cysteine (proteins)					0.2597	10.395
Ionic strength	9.3	1.7	8.3	25.4	11.41	144.4
Ca^{2+} + Mg^{2+}	1.66	0.24	2.50	1.11		0.62

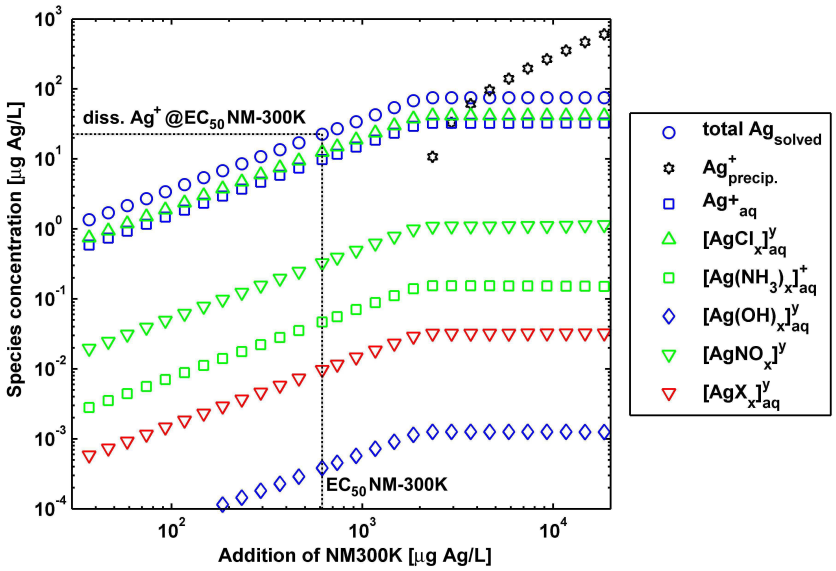

Fig. S8 Silver speciation of NM-300K in algae medium for Pseudokirchneriella (OECD 201). The dotted line represents the data for the EC_{50} of AgNP NM-300K.

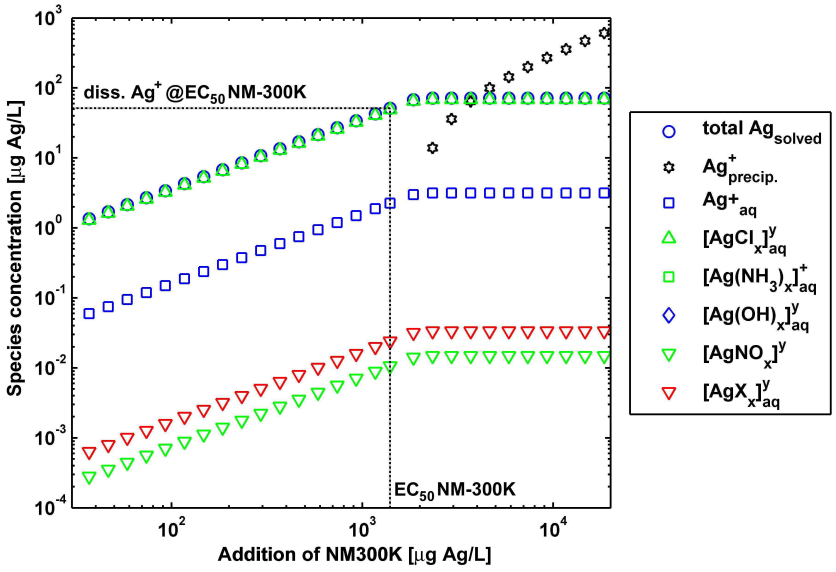

Fig. S9 Silver speciation of NM-300K in algae medium for Scenedesmus. The dotted line represents the data for the EC_{50} of AgNP NM-300K.

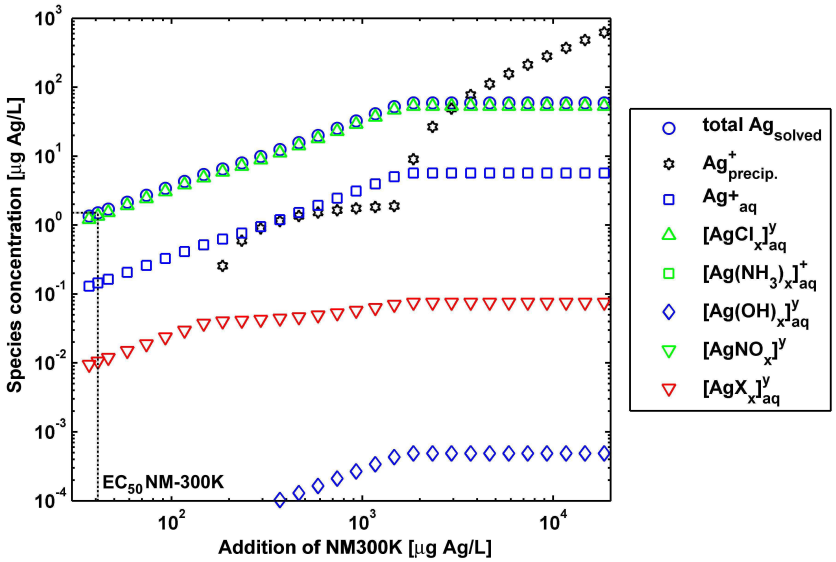

Fig. S10 Silver speciation of NM-300K in test medium for Daphnia (OECD 202). The dotted line represents the data for the EC_{50} of AgNP NM-300K.

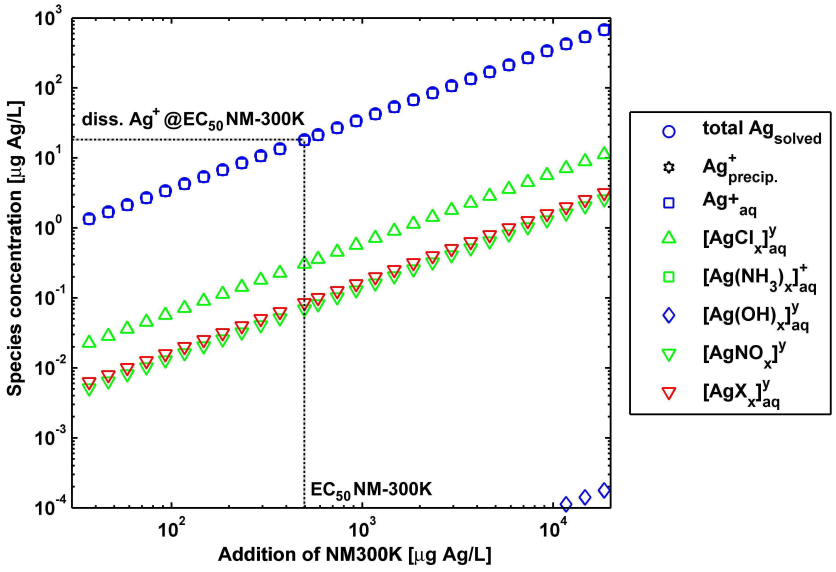

Fig. S11 Silver speciation of NM-300K in test medium for Lemna (OECD 221). The dotted line represents the data for the EC_{50} of AgNP NM-300K.

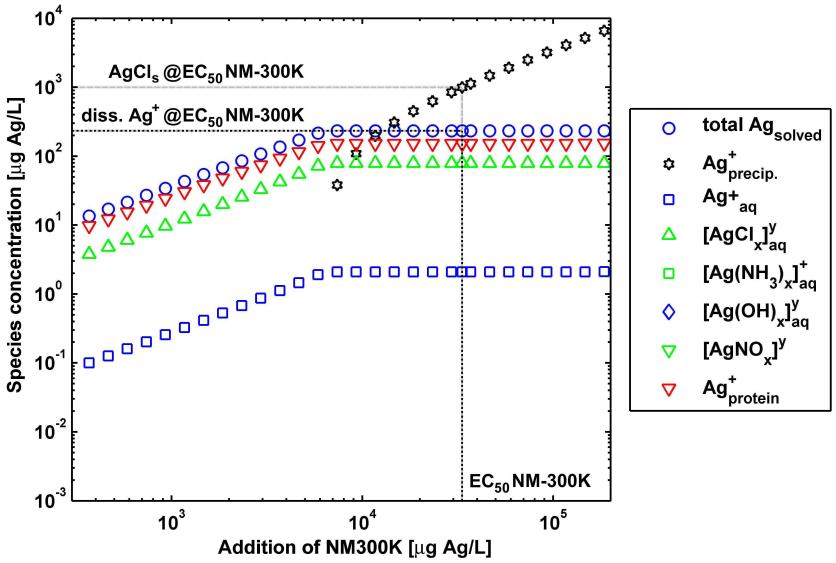

Fig. S12 Silver speciation of NM-300K in growth medium for Arthrobacter. The dotted line represents the data for the EC_{50} of AgNP NM-300K.

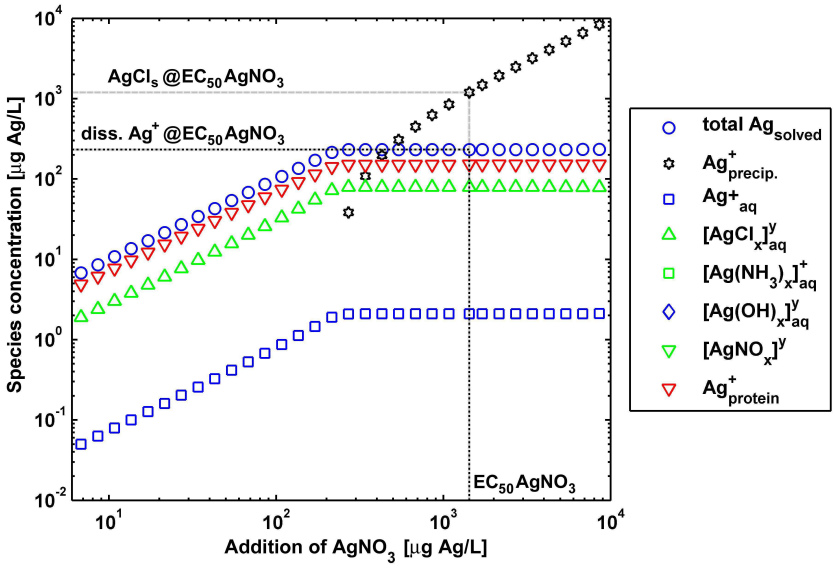

Fig. S13 Silver speciation of $AgNO_3$ in growth medium for Arthrobacter. The dotted line represents the data for the EC_{50} of $AgNO_3$.

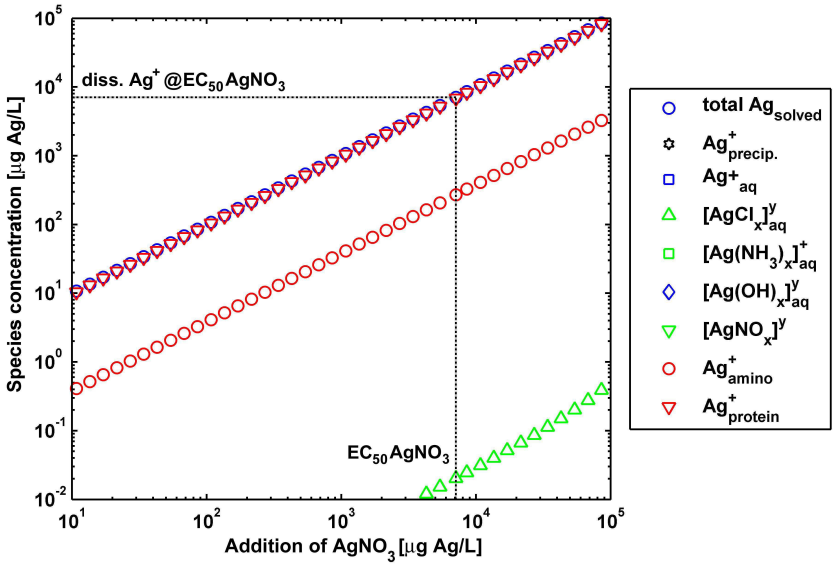

Fig. S14 Silver speciation of $AgNO_3$ in test medium for liver cells HepG2. The dotted line represents the data for the EC_{50} of $AgNO_3$.

Table S5 Experimental EC_{50} values ($\pm$ standard deviation) for NM-300K from literature for the test organisms related to the here investigated test media; data in ( )-brackets represent the confidence limits (95 %) of the EC_{50} determination. Using $AgNO_3$ EC_{50} as dissolved Ag concentration allowed for predicting reversely NM-300K EC_{50}. *Prediction considering also the colloidal species $AgCl_s$ (see text). Toxicity data for Desmodesmus, Danio rerio and Myriophyllum[18] was also used for EC_{50} prediction. The toxicity data for Desmod. (inhibition, biomass growth) were calculated as average $\pm$ standard deviation ($n = 4$). The toxicity data for Danio (lethality) were calculated as average $\pm$ standard deviation ($n = 5$). The toxicity data for Myrioph. (multiple endpoints) were calculated as average $\pm$ standard deviation ($n = 2$, average of all endpoints) for NM-300K and for $AgNO_3$ as average $\pm$ standard deviation ($n = 1$, average of all endpoints).

Test organism	$EC_{50,NM-300K}$ experimental [μg Ag/L]	$EC_{50,AgNO_3}$ experimental [μg Ag/L]	$EC_{50,NM-300K}$ predicted [μg Ag/L]
Pseudok.	617 ± 367[19]	16.1 ± 4.9[19]	436 ± 134
Scened.	1399 ± 540[19]	8.4 ± 3.2[19]	228 ± 86
Daphnia m.	41 ± 14[18]	2.3 ± 0.3[20]	63.1 ± 8.4
Lemna m.	496 (192 1105)[21]	31 (26 37)[22]	843 (707 1006)
Arthrob.	33380 (29940 38370)[23]	1430 (1210 1710)[23]	*38890 (32907 46505)
HepG2	$\gg$50000[19]	7080 ± 2410[19]	192550 ± 65542
Desmod.	33 ± 13[18]	2.1 ± 1.4[18]	57 ± 38
Danio r.	1000 ± 520[18]	71 (57 102)[18]	1931 (1550 2774)
Myrioph.	1438 ± 733[18]	38 ± 17[18]	1033 ± 463

Table S6 Comparison of the experimental speciation data for membrane filtration (MF) and ultracentrifugation (UC) with the numerical speciation approaches for Ag^+ binding to proteins. The deviation D_i of the numerical data (c_{num}) from the experimental data (c_{exp}) is calculated as $D_i = \sum_i |\log_{10} Q_i|$ with $Q_i = c_{num,i}/c_{exp,i}$. The numerical speciation approaches are as follows (see for details section of the main document): (1) only free cysteine; (2) BSA with 1 available cysteine-group and free cysteine; (3) BSA with 14 available cysteine-groups and free cysteine; (4) HSA with 14 strongly binding sites, 29 weakly binding sites (acc. to Shen *et al.*[24]) and free cysteine; (5) BSA with 1 binding site acc. to Zhao *et al.*[25]; (6) BSA with 13 available cysteine groups and free cysteine acc. to Rombouts *et al.*[26]; (7) BSA with 9 available cysteine groups and free cysteine acc. to Alexander & Hamilton[27].

Speciation approach	Ag^+ binding	Arthrob. [μmol/L]	HepG2 (w. 8% FCS) [μmol/L]	D_i Arthrob.	HepG2	$\sum$
Experimental speciation		$c_{exp,i}$				
MF	dissolved	0.5148	0.1378			
UC	dissolved & proteins	3.1728	5.5738			
Numerical speciation		$c_{num,i}$		D_i		
(1) Cys	dissolved	2.7020	2.7250	0.7898	1.6070	2.3967
	dissolved & proteins	2.7020	2.7250			
(2) BSACys1_Cys	dissolved	0.2480	0.7450	0.3870	1.0394	1.4264
	dissolved & proteins	2.7020	2.7520			
(3) BSACys14_Cys	dissolved	0.0179	0.0679	1.5287	0.6175	2.1462
	dissolved & proteins	2.7020	2.7590			
(4) HSA_Cys	dissolved	0.7092	2.7401	0.2089	1.6068	1.8157
	dissolved & proteins	2.7020	2.7410			
(5) BSA_Cys	dissolved	0.7541	2.7250	0.7885	1.6070	2.3955
	dissolved & proteins	0.7563	2.7250			
(6) BSACys13_Cys	dissolved	0.3540	0.0728	0.2324	0.5873	0.8197
	dissolved & proteins	2.7020	2.7290			
(7) BSACys9_Cys	dissolved	0.7090	0.1050	0.2087	0.4285	0.6372
	dissolved & proteins	2.7020	2.7280			

References

1 Deutsches Institut für Normung e.V., *DIN Richtlinie 38 406 Teil 18: Deutsche Einheitsverfahren zur Wasser-, Abwasser- und Schlammuntersuchung - Kationen (Gruppe E) - Bestimmung des gelösten Silbers durch Atomabsorptionsspektrometrie im Graphitrohrofen (E18)*, 1990.

2 E. M. Luther, Y. Koehler, J. Diendorf, M. Epple and R. Dringen, *Nanotechnology*, 2011, **22**, 375101.

3 W. Zhang, Y. Yao, N. Sullivan and Y. Chen, *Environmental Science & Technology*, 2011, **45**, 4422–4428.

4 H. Hagendorfer, R. Kaegi, M. Parlinska, B. Sinnet, C. Ludwig and A. Ulrich, *Analytical Chemistry*, 2012, **84**, 2678–2685.

5 R. Ma, C. Levard, S. M. Marinakos, Y. Cheng, J. Liu, F. M. Michel, G. E. Brown and G. V. Lowry, *Environmental Science & Technology*, 2012, **46**, 752–759.

6 B. C. Reinsch, C. Levard, Z. Li, R. Ma, A. Wise, K. B. Gregory, G. E. Brown and G. V. Lowry, *Environmental Science & Technology*, 2012, **46**, 6992–7000.

7 J. Dobias and R. Bernier-Latmani, *Environmental Science & Technology*, 2013, **47**, 4140–4146.

8 J. Liu, D. A. Sonshine, S. Shervani and R. H. Hurt, *ACS Nano*, 2010, **4**, 6903–6913.

9 B. Welz and M. Sperling, *Atomabsorptionsspektrometrie*, Wiley-VCH, Weinheim [u.a.], 4th edn., 1997.

10 P. S. Tourinho, C. A. van Gestel, K. Jurkschat, A. M. Soares and S. Loureiro, *Environmental Pollution*, 2015, **205**, 170–177.

11 D. J. Butcher and J. Sneddon, *A practical guide to graphite furnace atomic absorption spectrometry*, Wiley, New York [u.a.], 1998.

12 W. Slavin, D. Manning and G. Carnrick, *Talanta*, 1989, **36**, 171 – 178.

13 D. MacDougall and W. B. Crummett, *Anal. Chem.*, 1980, **52**, 2242–2249.

14 H. H. Ku, *Journal of Research of the National Bureau of Standards. Section C: Engineering and Instrumentation*, 1966, **70C**, 263–273.

15 D. A. Skoog and J. J. Leary, *Principles of instrumental analysis*, Saunders College Publishing, Orlando, 4th edn., 1992.

16 C. Spälti, *Messunsicherheit Volumen mittels Kolbenhubpipetten*, 2011, http://www.spaelti-ts.ch/pdf/genauigkeit_und_messunsicherheit_von_kolbenhubpipetten_d.pdf, (accessed January 2017).

17 D. Parkhurst, *PHREEQCi v3.3.7-11094*, 2016, http://wwwbrr.cr.usgs.gov/projects/GWC_coupled/phreeqci/, (accessed January 2017).

18 A. Lüdecke, C. Polleichtner and D. Völker, *Abschätzung der Umweltgefährdung durch Silber-Nanomaterialien: Vom chemischen Partikel bis zum technischen Produkt (UMSICHT), Schlussbericht Umweltbundesamt, Berlin & Dessau-Roßlau, Germany*, 2014, http://www.umsicht.uni-bremen.de/Abschlussberichte Partner/UBA Gesamtschlussbericht_UMSICHT_final mit Anlagen 1-3.pdf, (accessed January 2017).

19 J. Köser, M. Engelke, A. Kück, E. Lesnikov, J. Arning, J. Thöming and J. Filser, *Abschätzung der Umweltgefährdung durch Silber-Nanomaterialien: Vom chemischen Partikel bis zum technischen Produkt (UMSICHT), Abschlussbericht Universität Bremen, Germany*, 2013, http://www.umsicht.uni-bremen.de/Abschlussberichte Partner/Abschlussbericht_Uni_HB_2013-12-16_public.pdf, (accessed January 2017).

20 J. Baumann, Y. Sakka, C. Bertrand, J. Köser and J. Filser, *Environmental Science and Pollution Research*, 2014, **21**, 2201–2213.

21 D. Voelker, K. Schlich, L. Hohndorf, W. Koch, U. Kuehnen, C. Polleichtner, C. Kussatz and K. Hund-Rinke, *Environmental Research*, 2015, **140**, 661–672.

22 B. Naumann, M. Eberius and K.-J. Appenroth, *Journal of Plant Physiology*, 2007, **164**, 1656–1664.

23 M. Engelke, J. Köser, S. Hackmann, H. Zhang, L. Mädler and J. Filser, *Environmental Toxicology and Chemistry*, 2014, **33**, 1142–1147.

24 X.-C. Shen, H. Liang, J.-H. Guo, C. Song, X.-W. He and Y.-Z. Yuan, *Journal of Inorganic Biochemistry*, 2003, **95**, 124–130.

25 X. Zhao, R. Liu, Y. Teng and X. Liu, *Science of The Total Environment*, 2011, **409**, 892–897.

26 I. Rombouts, B. Lagrain, K. A. Scherf, M. A. Lambrecht, P. Koehler and J. A. Delcour, *Scientific Reports*, 2015, **5**, 12210.

27 P. Alexander and L. D. G. Hamilton, *Archives of Biochemistry and Biophysics*, 1960, **88**, 128–135.